RSC Advances

ROYAL SOCIETY OF CHEMISTRY

www.rsc.org/advances

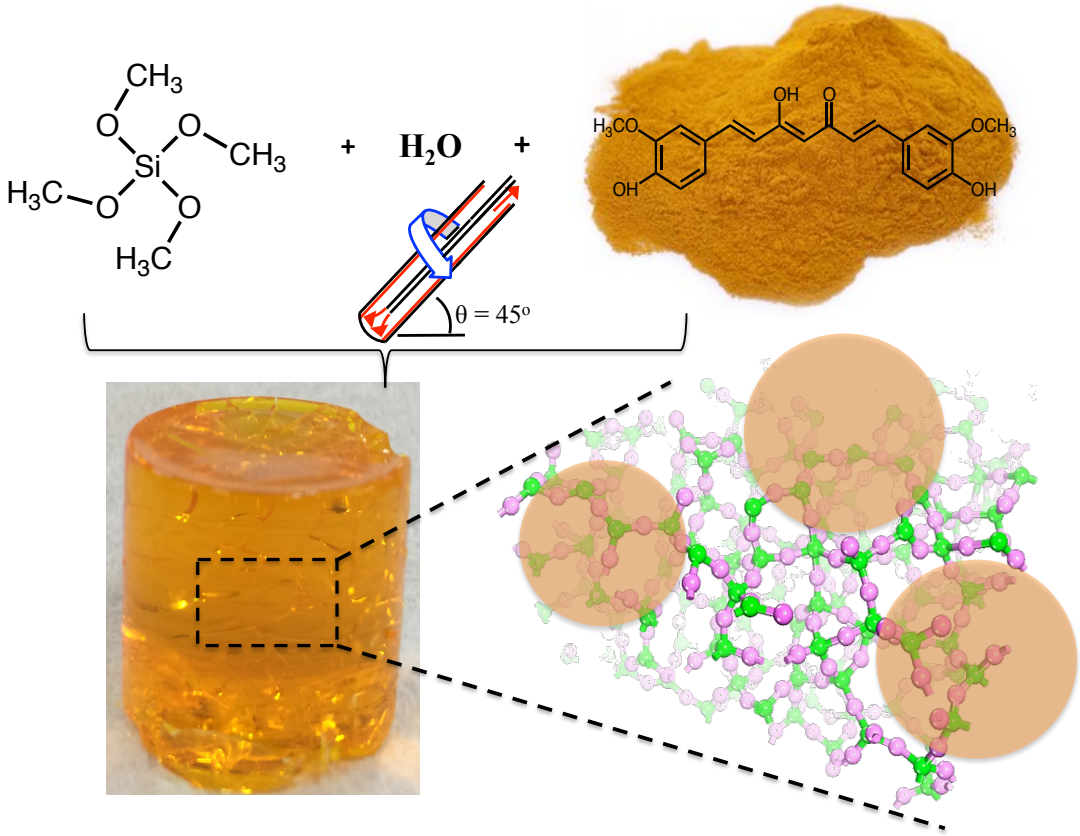

Sol-gel synthesis of silica xerogel using a continuous flow vortex fluidic device at room temperature is effective in direct incorporation of preformed cucumin particles, which has antimicrobial activity against *Staphylococcus aureus*.

RSC Advances

RSCPublishing

COMMUNICATION

Continuous flow vortex fluidic synthesis of silica xerogel as a delivery vehicle for curcumin†

Cite this: DOI: 10.1039/x0xx00000x

Chee Ling Tong[a] , Uwe H. Stroeher[b], Melissa H. Brown[b], and Colin L. Raston[a]*

Received 00th January 2012,
Accepted 00th January 2012

DOI: 10.1039/x0xx00000x

www.rsc.org/

Sol-gel synthesis of silica xerogel at room temperature is effective using a vortex fluidic device operating under scalable continuous flow conditions, using only tetramethyl orthosilicate as the silica precursor and deionized water. The gelation time of the hydrogel can be as short as 3.5 hours depending on the concentration of the silica. This process is also effective in incorporating preformed sub-micron particles of curcumin, as an effective vehicle for bioavailability of this compound, which was shown by antimicrobial activity against *Staphylococcus aureus*.

Solution-gelation ("sol-gel") technology has been known for decades and it is widely applied for fabricating silica materials. Tetraalkoxysilanes ($SiOR_4$) such as tetraethyl orthosilicate (TEOS) and tetramethyl orthosilicate (TMOS) are commonly used as precursors for preparing monolithic silica or silicate glasses,[1, 2] with the sol-gel reactions involving hydrolysis of alkoxysilanes, followed by room temperature condensation, which is summarized in equations (1–3).[3, 4]

Hydrolysis:

$$Si(OR)_4 + 4H_2O \rightarrow Si(OH)_4 + 4ROH \quad (1)$$

Alcohol condensation:

$$Si(OH)_4 + Si(OR)_4 \rightarrow (OH)_3Si–O–Si(OR)_3 + ROH \quad (2)$$

Water condensation:

$$Si(OH)_4 + Si(OH)_4 \rightarrow (OH)_3Si–O–Si(OH)_3 + H_2O \quad (3)$$

Alkoxysilanes are hydrophobic and are only sparingly soluble in water. In general they react slowly with water,[5] although this can be overcome in the presence of ethanol or methanol as a bridging medium. The sol-gel process involves lengthy hydrolysis and condensation, taking up to 1000 hours of gelation for TEOS,[1, 5] with the presence of acid or base speeding up the process.[4, 5] There is limited information available on producing either monolithic silica or silicate glasses without adding acid or base, while achieving a rapid gelation time with appreciable Brunauer–Emmett–Teller (BET) surface area and pore volume. Avnir *et.al.* established that rapid gelation of monolithic porous silica can be achieved without the addition of alcohol, however, no characterization data of the solid is available.[6] In addition, Dai *et.al.* established that no appreciable pore volume is present in the resulting silica material if only water is used as the reaction medium during the sol-gel process.[2]

Silicate glasses produced *via* sol-gel processing can be used in optical devices due to their excellent transparency,[7, 8] and as delivery vehicles for drugs,[9, 10] and biologically active molecules.[11] *In situ* synthesis of silica gel incorporating different compounds as such a delivery vehicle is challenging given the use of rather constraining conditions which feature in the hydrogel processing.[9] Typically, drug loading into silica is carried out as a multi-step batch process. For example, Smirnova *et.al.* have developed a 72 hour, two step synthesis of an aerogel involving the use of acid and base, followed by loading the drugs ketoprofen and griseofulvin under supercritical conditions.[9] Other compounds could also benefit from being incorporated into silica. The bioavailability of curcumin (Figure 1), which is derived from the plant *Curcuma longa*, is an ideal compound for incorporation. Curcumin has anti-cancer, anti-oxidant, anti-inflammatory, anti-bacterial, and anti-carcinogenic properties, and is often regarded as a model nutraceutical/molecular pharmaceutical for drug delivery applications.[12-17] Despite such remarkable properties, it suffers from low water solubility and bioavailability, and extreme sensitivity at physiological pH.[12, 13, 18] Zhao *et.al.* have developed a novel synthesis of mesoporous silica nanoparticles, for *in vivo* release of curcumin to zebrafish larvae, in developing a system for the treatment of heart failure.[17]

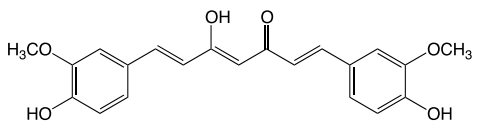

Figure 1. Chemical structure for curcumin.

Herein we establish the use of a recently developed vortex fluidic device (VFD),[11] for carrying out sol-gel processing at room temperature. This avoids the use of alcohol or an acid or base catalyst, with *in situ* incorporation of curcumin particles, which were preformed also using the VFD. The use of the VFD under scalable continuous flow conditions results in much faster kinetics, and offers scope for carrying out reactions under turbulent flow, beyond the limits of a diffusion control. Remarkably the use of the VFD imparts significant pore volume in the resulting silica, as judged by high BET surface area, in the absence of an organic solvent. Moreover, the use of the VFD avoids the inherent difficulty of traditional batch processing where uneven mass and heat transfer can result in non-uniform processing/products.[19, 20] Overall, the sol-gel processing in the present study is high in green chemistry metrics, in minimising the use of a solvent and auxiliary reagents, and operating the process at room temperature, which is an integral part of developing more benign processes in the anthropocene era.

We have previously established that ordered mesoporous silica is readily prepared using a VFD, also operating under continuous flow conditions, at room temperature, thus avoiding long hydrothermal processing times, with the intense shear in the dynamic thin film effective in controlling the pore size, as well as the pore wall thickness.[21] VFD is a versatile microfluidic platform, with processing capabilities also in controlling chemical reactivity and selectivity in organic synthesis,[20, 22, 23,24, 25] exfoliating graphene from graphite,[26] forming graphene-algae hybrid materials,[27, 28] controlling the growth of palladium nanoparticles on carbon nano-onions,[29] and controlling the polymorphs of calcium carbonate.[30]

In generating silica hydrogels, deionized Milli-Q water and TMOS were introduced into the base of a rapidly rotating glass tube (borosilicate NMR tube) inclined at an angle relative to the horizontal position via two separate feed jets (Figure 2). The high shear generated within the thin film in the VFD is able to overcome the otherwise immiscibility of the two liquids, indeed in forming what appears to be a single phase. This intense micro-mixing and the viscous drag as the liquid whirls up the tube facilitates the reaction, as does the the mechanoenergy within the Stewartson-Ekman layers arising from the liquid being driven up the rotating tube with gravity forcing the liquid back.[31] The inclination angle of the tube was set at 45 °, Figure 2, given that this has been shown to be the optimum angle for all the aforementioned applications of the VFD.

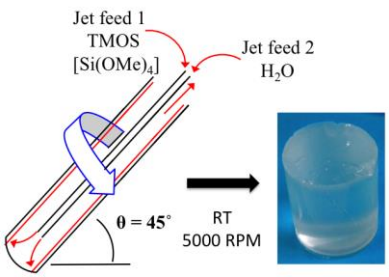

Figure 2. Schematics of the synthesis of the silica hydrogel.

Studies were undertaken on gelation time post VFD processing, for different silica to water molar ratios, as well as on the effect of using different rotational speeds for a 18.0 mm internal diameter glass tube housed in the VFD. At 5000 RPM, the time for gelation is the shortest regardless of the molar ratio, with overall gelation times consistently within 3 to 4 hours as judged visually, as opposed to most commonly used method, namely rheological measurements.[32] Typically in rheology measurement, the gelation time is recorded corresponding to the onset of gelation by the sudden increase of storage modulus, *G'*,[33] and visual judgement recorded in our study may be overstated. However, at higher rotational speed, changing the water to silica molar ratio affects the gelation time, with the optimum time at 6000 RPM and 7000 RPM corresponding to a H_2O/Si molar ratio of 10:1, Figure 3. The variation in gelation time associated with changing the H_2O/Si molar ratio and rotation speed is based on visual observations, noting that the fluid dynamics within the VFD are inherently complex. This is highlighted by our recent findings of a speed dependent vibration induced Faraday wave in the device which dramatically affects rates of reactions.[34] Nitrogen adsorption-desorption analyses show variation in BET surface area and Barrett–Joyner–Halenda (BJH) pore volume (Table 1). The BJH pore volume increased with an increase in water to TMOS molar ratio, and the trend was consistent for different rotational speeds. Overall the change in rotational speed for the process only affects the gelation time of the sample post VFD processing, whereas all the physisorption characteristics remained consistent with variation of the H_2O/Si molar ratio.

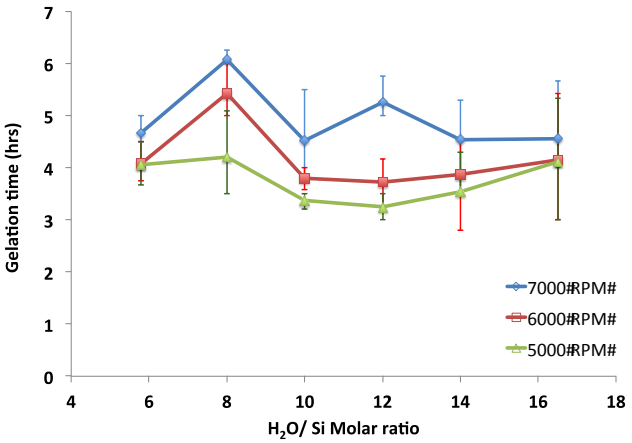

Figure 3. Change in gelation time at different H_2O/Si molar ratios for different rotational speeds (data points in triplicate).

Table 1. Physisorption properties of silica xerogels for different Si/H_2O molar ratios and different rotational speeds on the VFD.*

Si/H_2O (mol ratio)	5000 RPM		6000 RPM		7000 RPM	
	S_{BET} (m^2/g)	V_p (m^3/g)	S_{BET} (m^2/g)	V_p (m^3/g)	S_{BET} (m^2/g)	V_p (m^3/g)
1 : 6	646.5	0.39	605.1	0.35	591.3	0.38
1 : 8	590.7	0.32	565.4	0.31	578.0	0.32
1 : 10	566.1	0.31	612.1	0.34	616.4	0.34
1 : 12	624.7	0.35	646.6	0.36	649.6	0.36
1 : 14	718.6	0.40	713.2	0.40	729.6	0.40
1 : 16.5	764.1	0.48	752.4	0.44	804.1	0.48

* S_{BET}, BET total surface area determined from N_2 adsorption desorption; V_p, total pore volume determined from BJH adsorption at relative pressure of 0.996.

For comparing VFD and batch processing, a sample was prepared using conventional batch processing for the same molar ratio of water to silica at 8:1, with the TMOS and deionized Milli-Q water added into a round-bottom flask via two separate feed jets. The solution was stirred at room temperature for 8 min, and the onset of gelation was monitored, which was found to be in excess of 9 hours. The BET surface area of this sample is 459.8 m^2/g and pore volume of 0.25 cm^3/g, both being significantly less than for the material using VFD. FTIR spectra of this batch derived silica xerogel, and that derived from VFD processing, along with that of TMOS itself are shown in Figure S1. Both silica xerogel samples show common bands assigned to various vibrations in the gel network. The intense band at 1050 – 1200 cm^{-1} is assigned to Si–O–Si asymmetric

stretching vibrations. The symmetric stretching vibrations of Si–O–Si appears at 790 cm^{-1}, with the expected in-plane stretching vibrations of the silanols Si–OH groups at 940 cm^{-1}.[35, 36] Both samples were devoid of any peaks corresponding to –CH vibrations arising from incomplete hydrolysis and condensation. This is despite the short processing time using the VFD, where under continuous flow processing, the residence time for a finite amount of liquid moving along the tube is approximately 3 min. ^{29}Si NMR data show that the xerogel derived from using the VFD has 95% degree of condensation, which is higher compared to the batch process derived xerogel, at 89% (Figure S2), despite the dramatic difference in gelation time.

While curcumin is only sparingly soluble in water, it dissolves in organic solvents, and we used this property to form sub-micron size particles of the compound for subsequent incorporating into silica, and possibly for enhanced bioavailability. Initially the curcumin was dissolved in ethanol and introduced into the VFD through one jet feed with excess deionized water added through a second jet feed, also as a continuous flow process. The molar ratio of H_2O: ethanol was fixed at 8:1, with the resulting curcumin in the form of a colloidal suspended in the solvent mixture. Dynamic light scattering (DLS) gave a mean hydrodynamic diameter of 465 nm (Figure 4), which is consistent with the estimated particle sizes from scanning electron micrograph (SEM) ranging from 300 – 470 nm (Figure 5). Much smaller particles of curcumin ~50 nm in diameter, stabilised by surfactants, are accessible using related rotating tube processing, involving acid-base precipitation.[15] Amorphous spheroidal curcumin precipitates 30 – 40 nm in diameter have been prepared also using the anti-solvent approach with a micromixer, but they agglomerate into ca. 140 nm particles, eventually forming needle-shaped curcumin crystals.[37] This finding agrees with our x-ray powder diffraction (XRD) data, with the particles of curcumin formed using the anti-solvent approach on the VFD becoming crystalline on standing, but the curcumin particles embedded in silica immediately after fabrication remain amorphous (Figure S3).

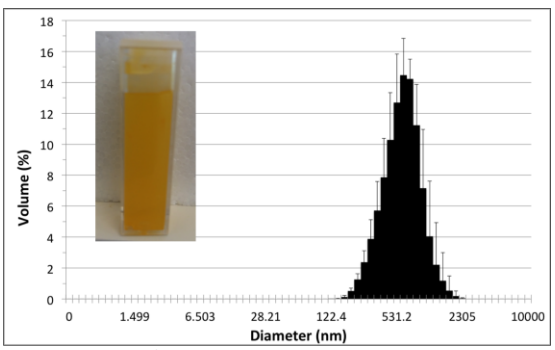

Figure 4. Bar graph of the particle sizes distribution with +/- 1 standard deviation error bars for curcumin particles suspended in Milli-Q water after VFD processing (inset).

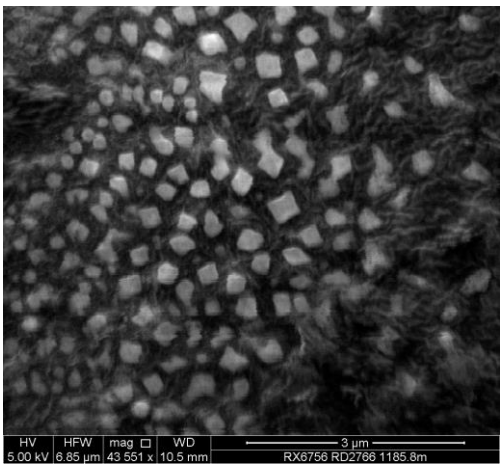

Figure 5. SEM image of curcumin particles prepared using the VFD. A suspension of the particles in deionized water was drop cast onto carbon tape and dried under air.

The colloidal suspension of curcumin was used to prepare composite silica hydrogel, using a similar procedure to that used for the material devoid of curcumin, as discussed above. TMOS was fed into the same VFD through one jet feed and the curcumin particles suspended in water in another jet fed, which served also as the aqueous medium for the hydrolysis and condensation of TMOS. The volumetric feed rate for these reactants was set at 0.6 mL/min. The molar ratio of H_2O/Si was fixed at 8:1, in order to compare the gelation time with the aforementioned silica gel synthesis. The samples were collected in a vial and allowed to stand at room temperature (~20 ˚C) for gelation. Further details on the procedure can be found in the supplementary information. The collected sample was clear orange with no obvious individual curcumin particles present (Figure S4(a)). Gelation time of this sample was 8 hours, with the longer gelation time presumably arising from the curcumin particles affecting the growth of silica network. The gel sample was then dried *in vacuo* at 60 ˚C to remove methanol generated during the synthesis of the silica, whereupon the material was ground using a mortar and pestle into a fine powder.

Fluorescence microscopy images identified the presence of curcumin particles, encapsulated within the silica network, and the particle size appears uniform (Figure 6). Encapsulation of curcumin in mesoporous silica with a multi-step self assembly approach has been reported by initially forming an aggregated micellar rods involving the use of surfactant, then loading the curcumin, and lastly hydrolysis of tetraethoxysilane under acidic conditions.[38] This material is effective in the controlled release of curcumin under physiological pH, with photo-stability of the compound within the silica matrix. In the present study, we explored the utility of the composite material for antibacterial activity based on the release of curcumin.[16, 39]

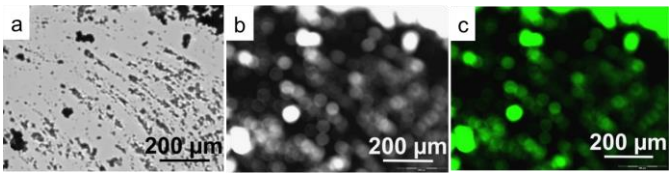

Figure 6. (a) Optical microscopy image of curcumin/SiO_2 composite material, (b) bright field image, and (c) fluorescence image.

The gram positive bacterium *Staphylococcus aureus* were grown overnight on Mueller Hinton agar at 37 ˚C. Fresh bacterial colonies were then inoculated into Mueller Hinton broth to give a final optical

density of 0.01 at an absorbance of 600 nm. Starting with 10^8 colony forming unit (cfu)/mL, bacterial cultures were serially diluted 1:10 into phosphate buffer saline (PBS) and 5 µL of the diluted OD 0.01 bacterial suspension was spotted onto the selective Mueller Hinton agar plates. The bacterial suspension was allowed to dry and the plates were incubated overnight (16 hrs) at 37 ˚C. Firstly, a control test was carried out to verify that silica xerogel has no effect on bacteria growth inhibition. Here 1 g of silica powder was added as a dry powder to 15 mL tubes and Mueller Hinton agar was added and mixed to give a final volume of 10 mL. Then 8 different concentrations of bacteria were spotted onto the surface and incubated. After 16 hours, bacterial growth was observed (Figure S5). This result indicated that the as-synthesized silica powder devoid of curcumin is non-toxic and has no antimicrobial capability.

We then prepared five different concentrations of curcumin/SiO_2 composite and curcumin sub micro-particles suspension (CNPS) for the same growth test. The concentration of the curcumin in the sample was determined using two different methods, fluorescence spectroscopy and simultaneous thermal analyser (STA), to compare the integrity of the analysis results. Interpolated data from a linear calibration curve using fluorescence spectroscopy gave 0.19% w/w curcumin in the composite sample (refer to ESI for the method of calculation). STA analysis revealed an endothermic peak at 172 ˚C in the differential scanning calorimetry (DSC) curve, which corresponds to the melt temperature of curcumin.[39, 40] Thermo-gravimetric analysis (TGA) gave 0.24 %w/w curcumin present in the composite material (Figure S6). Both results are reasonably consistent and the higher limit of 0.24% w/w was used for the determination of curcumin concentration in the composite sample for the bacterial growth inhibition test. Here 0.25 g, 0.50 g, 0,75 g, 1.0 g, and 1.25 g of curcumin/SiO_2 powder, with curcumin concentration of 60, 120, 180, 240 and 300 µg.mL^{-1} respectively, were added and mixed with the Mueller Hinton agar (left side of the Mueller Hinton agar plates) (Figure 7). On the right side, different concentrations of CPNS were prepared for performance comparison (Figure 7). The curcumin concentrations were 209, 418, 628, 838, and 1047 µg.mL^{-1} respectively (Figure 7). For the curcumin/SiO_2 sample, a partial inhibition of the bacterial growth is seen at curcumin concentrations as low as at 120 µg.mL^{-1} (Figure 7(b), left), with a more pronounced effect at a concentration of 180 and 240 µg.mL^{-1} (Figure 7 (c,d), left). Total growth inhibition is achieved at a concentration of 300 µg.mL^{-1} (Figure 7 (e), left). In contrast, the CNPS also showed mild inhibition starting at 628 µg.mL^{-1} (Figure 7 (c), right) and full inhibition at 1047 µg.mL^{-1} (Figure 7(e), right). Thus, the curcumin/SiO_2 composite outperformed the curcumin particles by four fold for the bacterial growth inhibition tests (Table S1). The improved inhibition of bacterial growth by curcumin in the composite material may be due to the silica network shielding the curcumin from degradation, prior to release/bioavailability. Alternatively, the porous network of silica enhances the absorption process, allowing the curcumin to slowly diffuse and thus, improves its bioavailability. The shielding is evident by comparing the same sample over a longer period of time. When the 1.0 g and 1.25 g samples were incubated for 48 hours, the bacterial grew fully on the CNPS whereas the curcumin/SiO_2 composite still showed growth inhibition at lower bacterial concentrations (Figure S7).

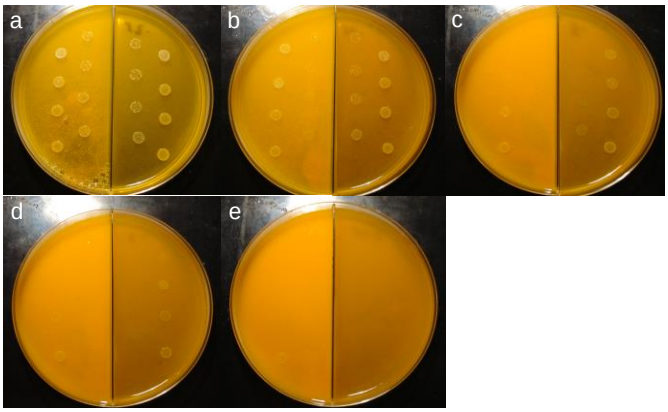

Figure 7. Bacterial growth inhibition test on a Mueller Hinton agar plates with curcumin/SiO_2 composite powder added on the left hand side, and CNPS added on the right hand side with (a) 60 / 209 µg.mL^{-1}, (b) 120 / 419 µg.mL^{-1}, (c) 180 / 628 µg.mL^{-1}, (d) 240 / 838 µg.mL^{-1}, and (e) 300 / 1047 µg.mL^{-1}.

Conclusions

We have developed a benign aqueous synthesis of silica hydrogel, which is without precedence in terms of a significantly reduced processing time, without the need for a solvent or the addition of an acid or base. Moreover, the same processing can be used for *in situ* incorporation of curcumin particles into the silica. This composite material showed better performance in bacterial growth inhibition compared to neat curcumin. The silica network appears to provide an excellent shielding to the curcumin particles, and better control in diffusion and thus improved bioavailability of this multi-medicinal functional compound. The simplicity of this process greatly promotes the use of silica as a drug delivery vehicle, in minimising the use of chemicals involved throughout the process. Future work can be done in substituting different drugs using the same procedure, along with the general application of the ability to make silica under more benign processing conditions, and presumably involving less energy input, while significantly reducing the generation of waste.

The composite material can be further functionalized by introducing different sources of silica precursor such as mercaptopropyl-trimethoxysilane, aminopropyltrimethoxysi-lane, and vinyltriehtoxysilane during the synthesis, in undergoing co-condensation, instead of post-grafting method. The silica hydrogel is hydrophilic due the –OH group on the surface, and functionalizing the surface of the silica will change the hydrophobicity of the material and thus expand the applications, which will be the focus of further studies.

The high surface tension of the pore liquid in the present study may lead to cracking and shrinkage during the drying process due to the capillary pressure and condensation of surface silanol groups.[40] However, this can be overcome by using supercritical CO_2 drying,[41, 42] solvent exchange,[42, 43] or liquid–paraffin–medium solvent evaporation.[44]

Support from the Government of South Australia, the Australian Research Council and National and Medical Research Council of Australia is gratefully acknowledged, as is Haniff Wahid's fluorescence microscopy help.

Notes and references
[a] Flinders Centre for NanoScale Science and Technology, School of Chemical and Physical Sciences, Flinders University, Bedford Park, SA 5042, Australia. *Fax: +618-8201-2905; Tel: +618-8201-7958; E-mail: colin.raston@flinders.edu.au*
[b] School of Biological Sciences, Flinders University, Bedford Park, SA 5042, Australia.

† Electronic Supplementary Information (ESI) available: Synthesis details and complete characterization data. See DOI: 10.1039/c000000x/

1. K. Kajihara, *J. Asian Ceram. Soc.*, 2013, **1**, 121-133.
2. S. Dai, Y. H. Ju, H. J. Gao, J. S. Lin, S. J. Pennycook and C. E. Barnes, *Chem. Comm.*, 2000, 243-244.
3. F. Surivet, M. Lam Thanh, J. P. Pascault and T. Pham Quang, *Macromolecules*, 1992, **25**, 4309-4320.
4. C. J. Brinker, *J. Non-Cryst. Solids*, 1988, **100**, 31-50.
5. M. A. Fardad, *J. Mater. Sci.*, 2000, **35**, 1835-1841.
6. D. Avnir and V. R. Kaufman, *J. Non-Cryst. Solids*, 1987, 92, 180-182.
7. M. C. Kyung, in *Optical Devices in Communication and Computation*, ed. P. Xi, InTech, 2012, ch. 10, p. 230.
8. R. Ciriminna, A. Fidalgo, V. Pandarus, F. Béland, L. M. Ilharco and M. Pagliaro, *Chem. Rev.*, 2013, **113**, 6592-6620.
9. I. Smirnova, S. Suttiruengwong and W. Arlt, *J. Non-Cryst. Solids*, 2004, **350**, 54-60.
10. U. Guenther, I. Smirnova and R. H. H. Neubert, *Eur. J. Pharm. Biopharm.*, 2008, **69**, 935-942.
11. S. Radin, S. Bhattacharyya and P. Ducheyne, *Acta Biomater.*, 2013, **9**, 7987-7995.
12. P. Anand, A. B. Kunnumakkara, R. A. Newman and B. B. Aggarwal, *Mol. Pharmaceutics*, 2007, **4**, 807-818.
13. M. M. Yallapu, M. Jaggi and S. C. Chauhan, *Drug Discovery Today*, 2012, **17**, 71-80.
14. S. Jambhrunkar, S. Karmakar, A. Popat, M. Yu and C. Yu, *RSC Adv.*, 2014, **4**, 709-712.
15. S. Dev, P. Prabhakaran, L. Filgueira, K. S. Iyer and C. L. Raston, *Nanoscale*, 2012, **4**, 2575-2579.
16. P. S. Negi, G. K. Jayaprakasha, L. Jagan Mohan Rao and K. K. Sakariah, *J. Agric. Food. Chem.*, 1999, **47**, 4297-4300.
17. H. Yan, C. Teh, S. Sreejith, L. Zhu, A. Kwok, W. Fang, X. Ma, K. T. Nguyen, V. Korzh and Y. Zhao, *Angew. Chem. Int. Ed.*, 2012, **51**, 8373-8377.
18. A. Goel, S. Jhurani and B. B. Aggarwal, *Mol. Nutr. Food Res.*, 2008, **52**, 1010-1030.
19. X. Chen, N. M. Smith, K. S. Iyer and C. L. Raston, *Chem. Soc. Rev.*, 2014, **43**, 1387-1399.
20. L. Yasmin, K. A. Stubbs and C. L. Raston, *Tetrahedron Lett.*, 2014, **55**, 2246-2248.
21. C. L. Tong, R. A. Boulos, C. Yu, K. S. Iyer and C. L. Raston, *RSC Adv.*, 2013, **3**, 18767-18770.
22. L. Yasmin, T. Coyle, K. A. Stubbs and C. L. Raston, *Chem. Comm.*, 2013, **49**, 10932-10934.
23. L. Yasmin, X. Chen, K. A. Stubbs and C. L. Raston, *Sci. Rep.*, 2013, 3.
24. L. Yasmin, P. K. Eggers, B. W. Skelton, K. A. Stubbs and C. L. Raston, *Green Chem.*, 2014, DOI: 10.1039/C4GC00881B.
25. M. N. Gandy, C. L. Raston and K. A. Stubbs, *Org. Biomol. Chem.*, 2014, **12**, 4594-4597.
26. X. Chen, J. F. Dobson and C. L. Raston, *Chem. Comm.*, 2012, **48**, 3703-3705.
27. M. H. Wahid, E. Eroglu, X. Chen, S. M. Smith and C. L. Raston, *RSC Adv.*, 2013, **3**, 8180-8183.
28. M. H. Wahid, E. Eroglu, X. Chen, S. M. Smith and C. L. Raston, *Green Chem.*, 2013, **15**, 650-655.
29. F. M. Yasin, R. A. Boulos, B. Y. Hong, A. Cornejo, K. S. Iyer, L. Gao, H. T. Chua and C. L. Raston, *Chem. Comm.*, 2012, **48**, 10102-10104.
30. R. A. Boulos, F. Zhang, E. S. Tjandra, A. D. Martin, D. Spagnoli and C. L. Raston, *Sci. Rep.*, 2014, 4.
31. D. A. Bennetts and L. M. Hocking, *Proc R Soc A*, 1973, **333**, 469-489.
32. A. Ponton, S. Warlus and P. Griesmar, *J. Colloid Interface Sci.*, 2002, **249**, 209-216.
33. C. Metin, K. Rankin and Q. Nguyen, *Appl Nanosci*, 2014, **4**, 93-101.
34. J. Britton, S. B. Dalziel and C. L. Raston, *RSC Adv.*, (RA-ART-10-2014-011777.R1).
35. R. Al-Oweini and H. El-Rassy, *J. Mol. Struct.*, 2009, **919**, 140-145.
36. M. Ochoa, L. Durães, A. Beja and A. Portugal, *J Sol-Gel Sci Technol*, 2012, **61**, 151-160.
37. Y. He, Y. Huang and Y. Cheng, *Cryst. Growth Des.*, 2010, **10**, 1021-1024.
38. N. W. Clifford, K. S. Iyer and C. L. Raston, *J. Mater. Chem.*, 2008, **18**, 162-165.
39. Bhawana, R. K. Basniwal, H. S. Buttar, V. K. Jain and N. Jain, *J. Agric. Food. Chem.*, 2011, **59**, 2056-2061.
40. S. Yun, H. Luo and Y. Gao, *RSC Adv.*, 2014, **4**, 4535-4542.
41. H. Tamon, T. Sone and M. Okazaki, *J. Colloid Interface Sci.*, 1997, **188**, 162-167.
42. P. B. Wagh, R. Begag, G. M. Pajonk, A. V. Rao and D. Haranath, *Mater. Chem. Phys.*, 1999, **57**, 214-218.
43. R. Miyamoto, Y. Ando, C. Kurusu, H.-z. Bai, K. Nakanishi and M. Ippommatsu, *J. Sep. Sci.*, 2013, **36**, 1890-1896.
44. H. Yang, Q. Shi, B. Tian, S. Xie, F. Zhang, Yan, B. Tu and D. Zhao, *Chem. Mater.*, 2003, **15**, 536-541.